



Pergamon

Materials Research Bulletin 36 (2001) 627–637

Materials
Research
Bulletin

Controlled synthesis of titanium dioxide nanoparticles in a modified diffusion flame reactor

Hee Dong Jang^{a,*}, Seong-Kil Kim^b

^a*Division of Materials Development, Korea Institute of Geology, Mining, and Materials, Taejeon, 305-350, Korea*

^b*R&D Center, Samhwa Paint Industry, Ansan, 425-110, Korea*

(Refereed)

Received 1 July 2000; accepted 10 October 2000

Abstract

Titanium dioxide (TiO₂) nanoparticles were synthesized by the oxidation of titanium tetrachloride (TiCl₄) in a modified diffusion flame reactor. The reactor utilized a multiport diffusion type burner composed of 5 concentric tubes. The flame configuration was (Ar + TiCl₄)/Ar/H₂/O₂/air producing several tens of grams of TiO₂ nanoparticles per hour. Flame characteristics of the diffusion flame at the modified burner outlet were investigated. TiCl₄ concentration and flow rates of combustion gases such as oxygen, hydrogen and air were chosen as key experimental variables for the control of the particle size and phase composition. TiO₂ nanoparticles ranged from 10 to 30 nm in average particle diameter, and the mass fraction of anatase synthesized was 40 to 80% in all experiments. © 2001 Elsevier Science Ltd. All rights reserved.

Keywords: A. Ceramics; B. Chemical synthesis; D. Crystal structure

1. Introduction

Particles smaller than several tens of nanometer in primary particle diameter are considered as nanoparticles. Titanium dioxide (TiO₂) nanoparticles shows high surface area per unit volume. This high value causes an increase of activity as a catalyst and greater sensitivity as a sensor. Titanium dioxide nanoparticles are used as a photocatalyst, in cosmetics for high

* Corresponding author. Fax: +82-42-861-9727.

E-mail address: hdjang@kigam.re.kr (H.D. Jang).

absorption of ultraviolet light, in toners and coating materials, etc [1]. TiO₂ nanoparticles are routinely produced by the gas-to-particle conversion in flame reactors because this method provides good control of particle size, particle crystal structure and purity [2]. The diffusion flame that exhibits strong gradients in concentration and temperature during particle formation and growth is one of the interesting tool among the various flames to synthesize TiO₂ nanoparticles. Formenti et al. [3] have reported the production of TiO₂ nanoparticles by the oxidation of titanium tetrachloride (TiCl₄) in (O₂ + TiCl₄)/N₂/H₂/O₂ diffusion flames. They produced 6 to 145 nm sized anatase particles by varying the flow rate of TiCl₄ and that of oxygen carrying out TiCl₄ vapor. Vemury and Pratsinis [4,5] investigated the effect of dopants (SiCl₄, SnCl₂ and AlCl₃) and electric discharge (corona) on the particle size and phase composition of TiO₂ nanoparticles at the diffusion flame configuration of (Ar + TiCl₄)/air/CH₄. SiCl₄ decreased primary particle size and inhibited the transformation of anatase to rutile. Meanwhile, SnCl₂ and AlCl₃ were found to enhance the transformation of anatase to rutile. The corona discharge also showed same effect as the effect of SiCl₄ on the particle size and phase composition of TiO₂ nanoparticles. Pratsinis et al. [6] reported the effect of flame configurations such as (Ar + TiCl₄)/CH₄/O₂, (Ar + TiCl₄)/O₂/CH₄, etc on the specific surface area and phase composition of the TiO₂ nanoparticles in a diffusion flame reactor. Yang et al. [7] also used (air + titanium isopropoxide)/CH₄/O₂ diffusion flames for processing TiO₂ nanoparticles from titanium isopropoxide. TiO₂ particles obtained in their experiments were 5.2 to 11.0 nm in crystal size and 64 to 100% in anatase mass fraction. Although those previous studies have obtained a many interesting and important results, more studies on the characteristics of the formation, growth and phase transformation of TiO₂ nanoparticles in the diffusion flame are still required because the flame has complex environments. There are many variables for the synthesis of nanoparticles in the flames such as the configurations of the flame, the concentration of precursor, gas composition, gas flow rate, etc. Those parameters affect the flame characteristics, particle formation, particle aggregation, sintering, and phase composition of particles.

The standard diffusion flame having a configuration of precursor/fuel/oxidant has been most frequently used to synthesize particles by the gas phase reaction in the previous studies. But as Pratsinis et al. [6] have reported, the different flame configuration has great effect on the particle size and phase composition of TiO₂ nanoparticles. In this respect, the development of the well-designed burner having a specific flame configuration is very important and can be considered as know-how because it gives the best reaction condition of the precursor in the flame such as optimum temperature profile with feasible consumption of oxidant gas, stable flame for the optimum residence time of precursor, etc.

In the present study, the flame synthesis of TiO₂ nanoparticles with a modified diffusion flame reactor having a different flame configuration from the previous ones is presented and discussed. The modified diffusion flame reactor was prepared using the multiport burner that was composed of 5 concentric tubes, and the flame configuration was (Ar + TiCl₄)/Ar/H₂/O₂/air. A modified diffusion flame reactor was designed as a bench scale to produce more than several tens of grams of TiO₂ nanoparticles from TiCl₄ per hour, which was about ten times higher than previous studies. The advantage of the proposed flame is able to introduce large flow of air into the fifth tube of the multiport burner for minimizing the amount of pure oxygen, keeping low concentration of TiCl₄ and short residence time of TiCl₄ in the flame.

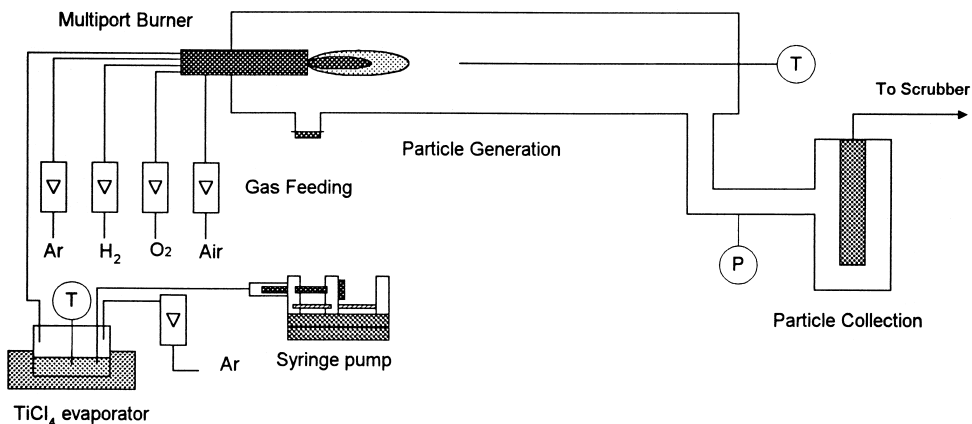


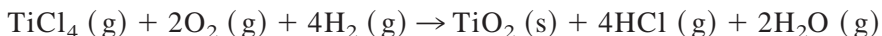
Fig. 1. A Schematic of experimental apparatus for the synthesis of TiO₂ nanoparticles.

Another merit of the flame is that it can introduce inert gases such as argon into the second tube of the burner to prevent plugging of the exit of precursor due to the deposition of the particles.

For the controlled synthesis of TiO₂ nanoparticles by the modified flame reactor TiCl₄ concentration, and the maximum flame temperature that depends on gas composition and flow rates of combustion gases in the modified diffusion flame reactor were chosen as key experimental variables. Effects of those variables on the particle diameter and phase composition were investigated.

2. Experiments

The overall reaction for the vapor-phase synthesis of TiO₂ from TiCl₄ in the present study is as follows;



A schematic of the bench-scaled experimental apparatus for the generation of TiO₂ nanoparticles is shown in Fig. 1. The experimental apparatus consists of an evaporator of aerosol precursor, an aerosol generator, and a particle collector.

A modified diffusion flame burner (3.4 cm in outside diameter and 45 cm in length) composed of five concentric stainless tubes (10, 16, 22, 28, and 34 mm in outside diameter) was prepared since it provided a stable flame over a wide range of operating conditions. Reactants mixing configuration of the aerosol generator is shown in Fig. 2. A quartz tube of 10 cm in diameter and 120 cm in length was installed to preserve the flame and particles. Liquid phase TiCl₄ was injected to the evaporator by using the syringe pump, and the vaporized TiCl₄ was carried into the central tube of the burner by introducing dry argon (Ar) gas (99.999%). The burner and manifold were kept about 20°C above the evaporator temperature to prevent condensation of TiCl₄ in the lines. Hydrogen (H₂) was used as a fuel while oxygen (O₂) and air were used as oxidants.

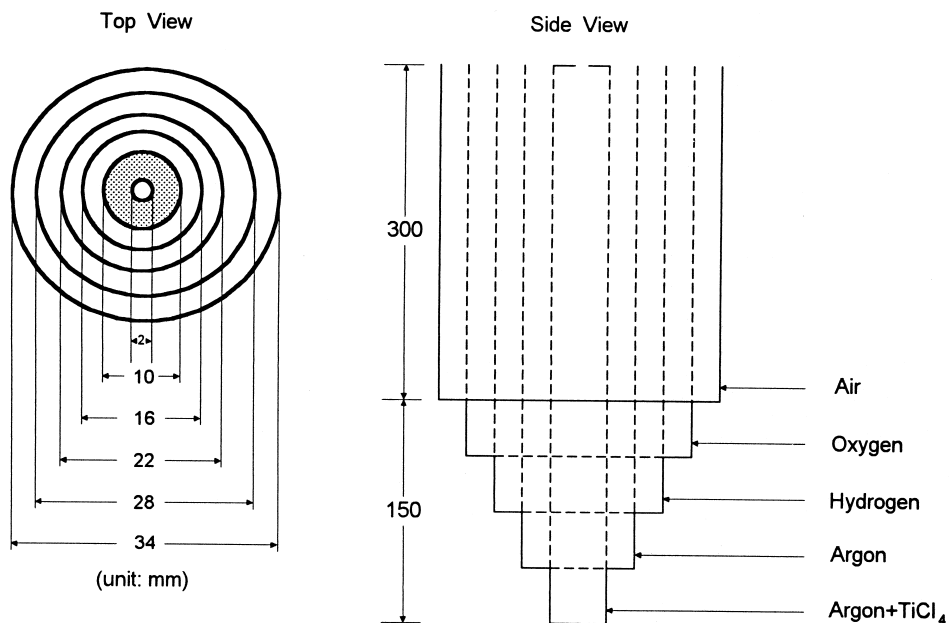


Fig. 2. Reactants mixing configuration of the aerosol generator (Remark: Shaded area at the top view of the burner is the reducer of outlet diameter of 1st tube).

A Pt-Rh R type thermocouple (Omega Engineering) was used to measure the flame temperature of the burner. The measurements were performed three times for each condition, and mean values were chosen as the flame temperatures in the axial direction of the flame in the absence of the precursor.

TiO₂ nanoparticles generated from TiCl₄ by the gas phase reaction were collected with a bag filter that was made of teflon fiber (Tefaire, Dupont Co.). The particle morphology and size were characterized by transmission electron microscopy (TEM, Philips Model CM12). The average particle diameter was determined by counting more than 200 particles from TEM pictures. The specific surface area of the powders was measured by nitrogen adsorption at -196°C using the BET equation (Micrometrics Model ASAP 2400). Assuming spherical particles, the average particle size d_p was calculated from measured specific surface area A and particle density ρ_p by $d_p = 6/(\rho_p \cdot A)$, and calculated particle sizes and observed ones were compared. X-ray diffractometer (XRD, Rigaku Co. Model RTP 300 RC) was used to obtain X-ray diffraction patterns of powders. The phase composition of TiO₂ particles was calculated from the relative intensities of the strongest peaks corresponding to anatase and rutile [8].

3. Results and discussion

3.1. Flame characteristics

Characteristics of the modified diffusion flame were investigated without introducing the TiCl₄ vapor into the burner. Flow rate of each tube was as follows; 1st: 2 l/min of Ar, 2nd:

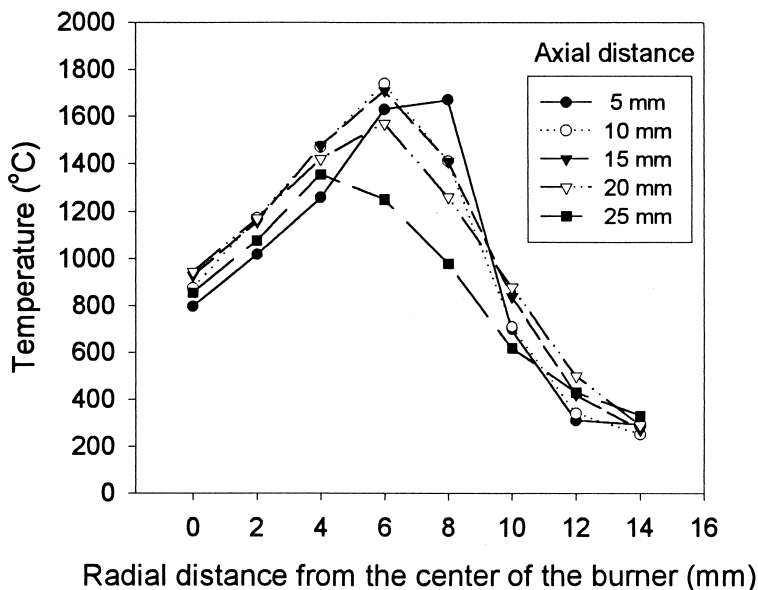


Fig. 3. Temperature distribution along axial direction of the diffusion flame.

5 l/min of Ar, 3rd: 6 l/min of H₂, 4th: 15 l/min of O₂, and 5th: 60 l/min of air. Fig. 3 shows the temperature distribution of the flame along the axial distance at different radial position. The temperature profiles having maximum at the different axial distance are found and the highest temperature in the flame is 1700°C, while the radial distance of the flame is 6 mm and axial distance of that is 10 mm. The adiabatic flame temperature from the thermodynamic calculation is about 2,000°C at same condition. The maximum temperature of the flame rapidly decreased from 1,700 to 1,300°C as the distance from the burner outlet increased from 5 to 25 mm. The height of the flame was about 6cm.

3.2. Effect of precursor concentration

The effect of precursor (TiCl₄) concentration in the flame synthesis on the primary particle size was investigated. TiCl₄ concentration in the flame was varied from 1.13×10^{-5} to 4.54×10^{-5} mol/l [9] by changing the feed rate of TiCl₄ at the maximum flame temperature of 1700°C, holding the gas flow rate as shown in Fig. 3. Fig. 4 shows change of the specific surface area of TiO₂ nanoparticles from BET analysis. As TiCl₄ concentration increased, the specific surface area decreased from 79 to 57 m²/g. The average diameter from the BET analysis was 19nm at 1.13×10^{-5} mol/l and increased to 28 nm at 4.54×10^{-5} mol/l. Fig. 5 shows the TEM pictures of TiO₂ nanoparticles made in the diffusion flame at the condition of Fig. 3. The average diameter from the TEM pictures was about 20 nm at the concentration of 1.13×10^{-5} mol/l and increased to about 30 nm by increasing the concentration to 4.54×10^{-5} mol/l. But the size distribution of TiO₂ nanoparticles became polydisperse as the concentration increased. The average particle sizes calculated from BET-adsorption areas

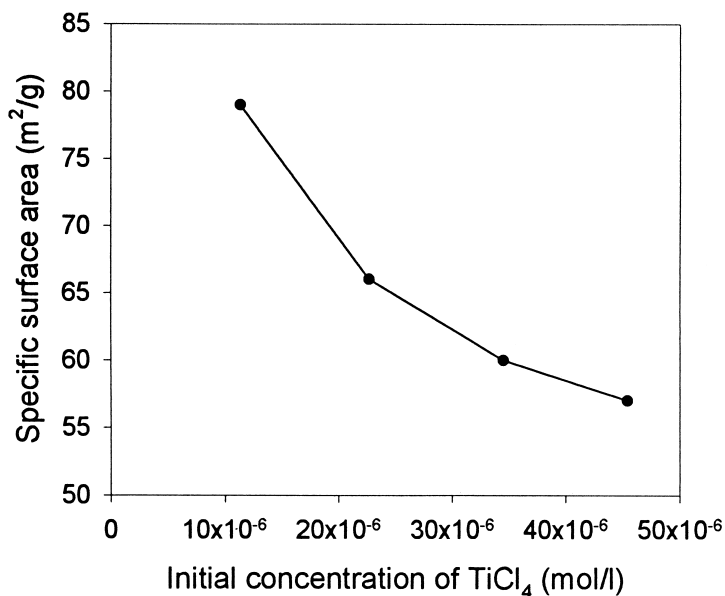


Fig. 4. Effect of TiCl₄ concentration on BET surface area (O₂: 15 l/min, Air: 60 l/min, H₂: 6 l/min, and Ar: 5 l/min, Carrier gas (Ar): 2 l/min).

were nearly the same as obtained from TEM study. The amount of collected particles at 4.54×10^{-5} mol/l of the TiCl₄ concentration was about 20 grams per hour. Plugging at the exit of the burner was not observed through the experiments. These results suggest that the synthesis of TiO₂ nanoparticles with the production rate of several tens of grams per hour was successful with the modified flame configuration in the present study.

As the concentration of aerosol precursor increases at the fixed flame temperature and gas glow rate, the growth rate of nuclei by the coagulation and surface reaction becomes faster than the nucleation rate during the gas phase reaction. Thus, larger primary particles are expected to be generated at the higher precursor concentrations [10]. Nanometer-sized primary particles form aggregates in the gas phase because of interactive forces between particles. Such aggregates change into large particles when the temperature in the gas phase is high enough to sinter the aggregates [11,12]. As can be seen in Fig. 5, the increase in the number of larger particles with TiCl₄ concentration appears to indicate that they are produced by the sintering. However, numerous smaller particles that seemed to be grown by the coagulation and surface reaction are observed at the low TiCl₄ concentration. If the sintering is dominant in the particle growth, it is expected that there should be many large particles at the low TiCl₄ concentration because the primary particle size is comparatively small at the low TiCl₄ concentration. Therefore, it is suggested that particle growth by the sintering is not dominant, and is only effective at the higher TiCl₄ concentrations in the present experimental condition.

From the analysis of X-ray diffraction patterns the crystalline phases of the TiO₂ nanoparticles generated from different TiCl₄ concentrations were found nearly same; it was about 45% anatase in mass fraction. The residence time at the condition of Fig. 3 is 0.033 sec that

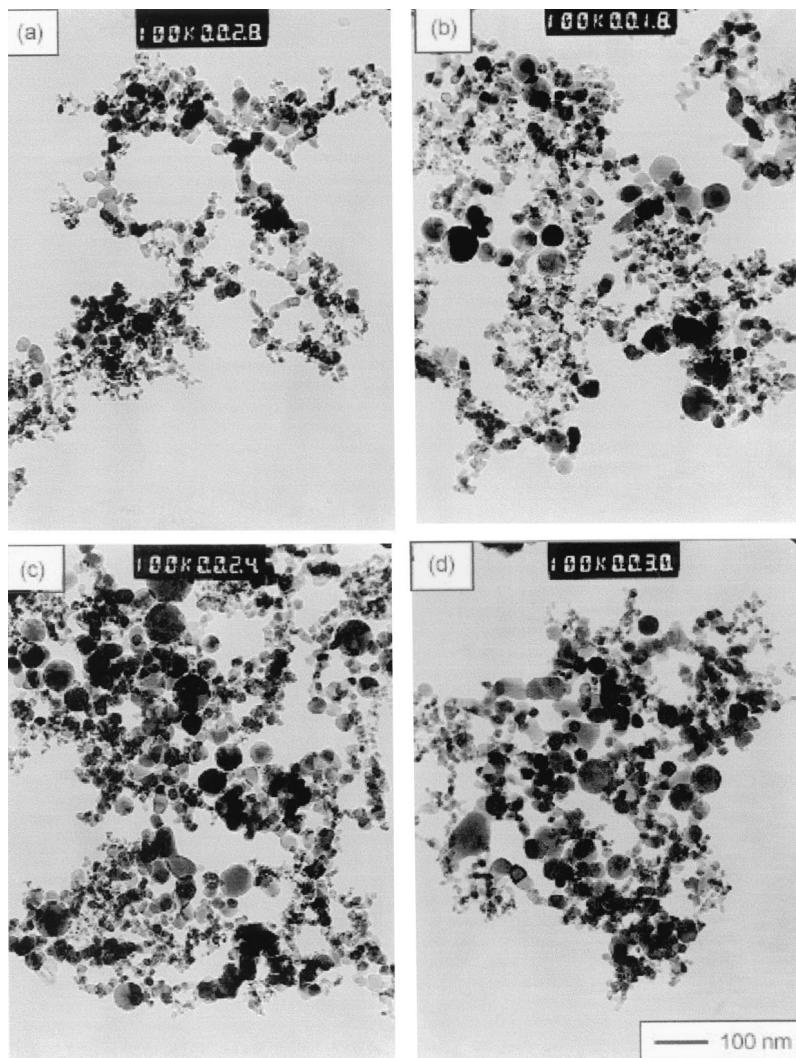


Fig. 5. TEM micrographs of TiO_2 nanoparticles collected at four different TiCl_4 concentrations (a: 1.13×10^{-5} , b: 2.27×10^{-5} , c: 3.45×10^{-5} , d: 4.54×10^{-5} mol/l).

is a little longer than those reported by Yang et al. [7]. The increase in residence time of reactant in the flame may increase the conversion rate of TiO_2 particles from anatase to rutile phase.

3.3. Effect of the maximum flame temperature.

The maximum flame temperature is also one of the very important variable for the determination of the particle size and crystal structure in the flame synthesis of TiO_2 nanoparticles. For the control of the maximum flame temperature, the flow rates of combustion gases such as oxygen, hydrogen and air were varied in the present study.

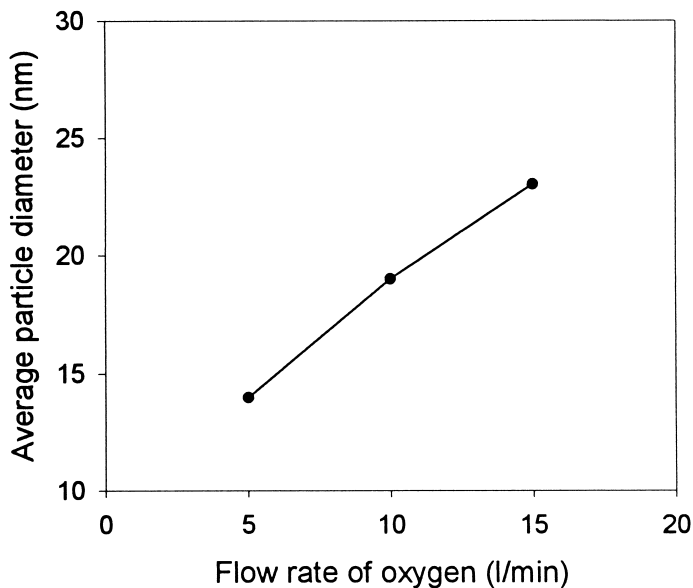


Fig. 6. Effect of pure oxygen flow rate of 4th tube on the product particle size.

The maximum temperature of the diffusion flame decreases as the oxygen flow rate decreases. Thus, the growth rate of particles due to low coagulation and sintering rates that are proportional to the temperature decreases resulting in smaller particles. Oxygen flow rate at the 4th tube of the burner decreased from 15 to 5 l/min with holding the gas flow rates of Fig. 3, and 2.27×10^{-5} mol/l of TiCl_4 concentration. As the oxygen flow rate decreased from 15 to 5 l/min, the air flow rate at the 5th tube increased from 60 to 75 l/min to keep the constant total gas flow rate; it means that TiCl_4 concentrations are the same in the flame. When the maximum flame temperature was lowered from 1700 to 1400°C along with the decrease of the oxygen flow rate, the average particle diameter calculated from the BET data also decreased from 23 to 14 nm (Fig. 6). This decrease of particle diameter in the present study is considered to be due to low coagulation and sintering rate of particles caused by the decrease in the temperature of diffusion flame.

The anatase mass fraction of TiO_2 nanoparticles increased from 41 to 80% as the oxygen flow rate decreased from 15 to 5 l/min (Fig. 7). The increase of the anatase mass fraction of TiO_2 nanoparticles is considered to be due to low transformation rate from anatase to rutile at the lower flame temperatures.

The flame temperature is also dependent on the hydrogen flow rate. As the hydrogen flow rate decreases, the flame temperature decreases rapidly and smaller particles are generated because of low coagulation and sintering rate in the flame. Higher mass fraction of anatase is also expected at lower flame temperature. Effect of hydrogen gas flow rate on the particle size and phase composition was investigated in the present study. Hydrogen flow rate at the 3th tube of the burner decreased from 8 to 4 l/min with holding the Ar flow rates (2nd tube) at 5 l/min, air flow rate (4th tube) at 10 l/min, air flow rate (5th tube) at 65 l/min, and TiCl_4 concentration at 2.27×10^{-5} mol/l. The air at the 4th tube was introduced instead of oxygen

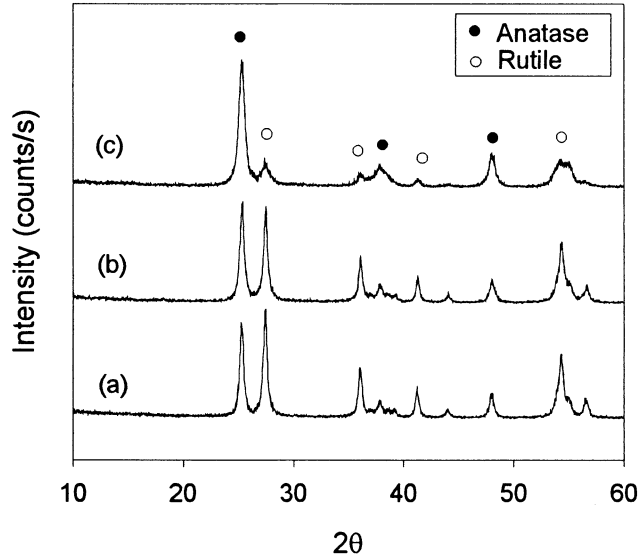


Fig. 7. X-ray diffraction patterns of TiO₂ particles showing the increase in the mass fraction of anatase with oxygen flow rate (a: 15, b: 10, c: 5 l/min).

to decrease the flame temperature and to minimize the production cost without using pure oxygen gas. With the decrease in hydrogen flow rate the maximum flame temperature was decreased from 1300 to 1000°C, and then the average particle diameter also decreased from 29 to 12 nm (Fig. 8). The anatase mass fraction increased from 27% at 8 l/min to 75% at

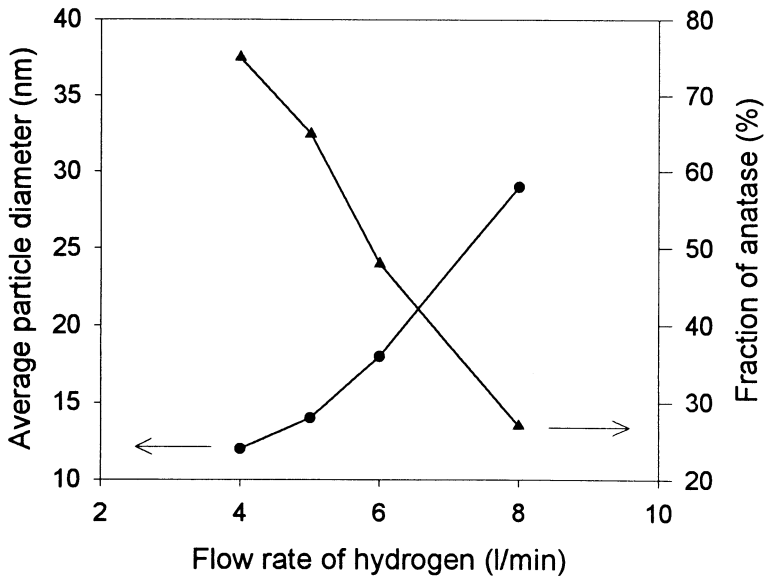


Fig. 8. Effect of hydrogen flow rate on the product particle size and mass fraction of anatase.

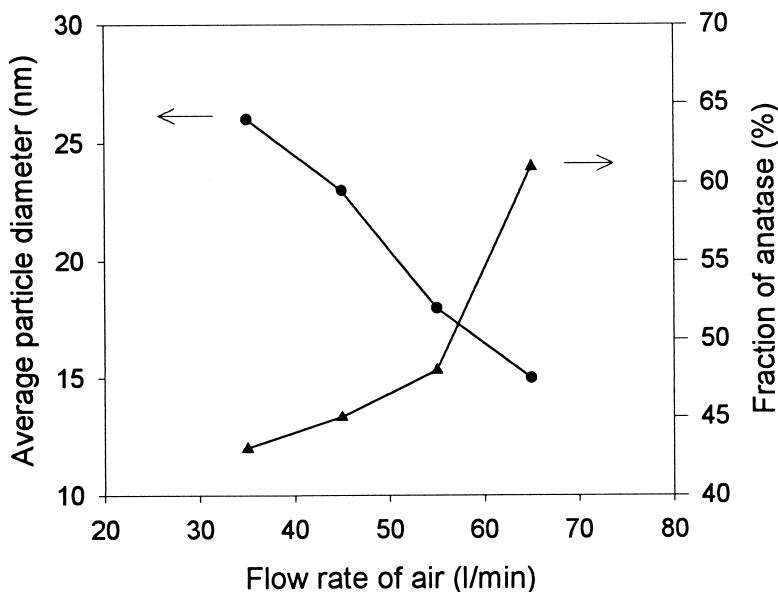


Fig. 9. Effect of total gas flow rate on the product particle size and mass fraction of anatase.

4 l/min (Fig. 8). The decrease in the particle size and increase in the anatase mass fraction of TiO_2 nanoparticles were thus obtained as expected.

Total gas flow rate was changed from 65 to 35 l/min by only decreasing the air flow rate at 5th tube of the burner. TiCl_4 feed rate at 2.0×10^{-3} mol/min, Ar at 5 l/min, H_2 at 6 l/min, air at 10 l/min and air at 65 l/min was the initial operating condition. As the air flow rate decreased, the adiabatic flame temperature from the thermodynamic calculation increased from 1,650 to 2,500°C. The TiCl_4 concentration in the flame increased from 1.38×10^{-4} to 1.91×10^{-4} mol/l with the decrease of air flow rate. Such increases of the flame temperature and TiCl_4 concentration were expected to result in the increase of particle size and decrease of anatase mass fraction of TiO_2 nanoparticles due to high coagulation rate of small particles. Average particle diameter increased from 15 to 26 nm (Fig. 9). As the flame temperature increased, large spherical particles produced by high sintering rate between small particles were also observed frequently in TEM analysis. Fig. 9 also showed the variation of the crystalline phase of TiO_2 nanoparticles generated at different total gas flow rates in the flame; it was 61% in anatase mass fraction at 65 l/min, and 43% at 35 l/min. Such increases of particle size and decrease of anatase mass fraction of TiO_2 nanoparticles are considered to be due to increase of the flame temperature, the TiCl_4 concentration and the residence time as expected.

4. Conclusions

Formation of TiO_2 nanoparticles from TiCl_4 was investigated in the modified diffusion flame reactor. Temperature distribution having maximum along the axial distance at the

different radial position of the flame was found. The highest production rate of TiO₂ nanoparticles using the modified flame reactor was about 20 grams per hour. As the TiCl₄ concentration increased from 1.13×10^{-5} to 4.54×10^{-5} mol/l, average particle diameter increased from 19 to 28 nm. When the maximum flame temperature was varied from 1700 to 1400°C by reducing oxygen flow rate from 15 to 5 l/min, the average particle diameter decreased from 23 to 14 nm, and the anatase mass fraction of TiO₂ nanoparticles was increased from 41 to 80%. The decrease in the hydrogen flow rate resulted in the lowering of the maximum flame temperature from 1300 to 1000°C, and subsequent reduction of the average particle diameter from 29 to 12 nm. The anatase mass fraction decreased with hydrogen flow rate from 75% at 4 l/min to 27% at 8 l/min. As the total gas flow rate was reduced from 65 to 35 l/min, the average particle diameter increased from 15 to 26 nm, and the crystalline phase of TiO₂ nanoparticles decreased from 61 to 43% in anatase mass fraction.

Acknowledgements

This study was supported by the Korea Institute of Industrial Technology Evaluation & Planning.

References

- [1] R.W. Siegel, *Nanophase Materials: Synthesis, Structure, and Properties*, F.F. Fujita (Ed.), Springer Series in Material Science, Springer-Verlag, Vol. 27, 1994, pp. 65.
- [2] A. Gurav, T. Kodas, T. Pluym, Y. Xiong, *Aerosol Sci. Technol.* 19 (1993) 411.
- [3] M. Formenti, F. Juillet, P. Meriaudeau, S.J. Teichner, P. Vergnon, *J. Colloid and Interface Science* 39 (1972) 79.
- [4] S. Vemury, S.E. Pratsinis, *J. Am. Ceram. Soc.* 78 (1995) 2984.
- [5] S. Vemury, S.E. Pratsinis, *Appl. Phys. Lett.* 66 (1995) 3275.
- [6] S.E. Pratsinis, W. Zhu, S. Vemury, *Powder Technol.* 86 (1996) 87.
- [7] G. Yang, H. Zhuang, P. Biswas, *Nanostructured Materials* 7 (1996) 675.
- [8] R.A. Spurr, H. Myers, *Anal. Chem.* 29 (1957) 760.
- [9] H.D. Jang, J. Jeong, *Aerosol Sci. Technol.* 23 (1995) 553.
- [10] S.K. Friedlander, *Smoke, Dust and Haze*, Wiley, New York, 1977, pp. 234.
- [11] T. Seto, M. Shimata, K. Okuyama, *Aerosol Sci. Technol.* 23 (1995) 183.
- [12] H.D. Jang, S.K. Friedlander, *Aerosol Sci. Technol.* 29 (1998) 81.